Journal of
Ceramic Science
and Technology

*J. Ceram. Sci. Tech.*, 08 [01] 155-160 (2017)
DOI: 10.4416/JCST2016-00104
available online at: http://www.ceramic-science.com
© 2017 Göller Verlag

# Droplet-Based Additive Manufacturing of Hard Metal Components by Thermoplastic 3D Printing (T3DP)

**U. Scheithauer[*], J. Pötschke, S. Weingarten,
E. Schwarzer, A. Vornberger, T. Moritz, A. Michaelis**

Fraunhofer IKTS, Institute for Ceramic Technologies and Systems,
Winterbergstrasse 28, D-01277 Dresden, Germany

received November 5, 2016; received in revised form December 25, 2016; accepted January 31, 2017

---

## Abstract

**Thermoplastic 3D printing (T3DP) is an Additive Manufacturing (AM) technology that cannot only be used for producing ceramic, metal or multi-material components, but for the Additive Manufacturing of hard metal or cemented carbide components, too. This is possible because the technology combines the precise deposition of small droplets of molten thermoplastic hard-metal-containing suspensions and an increasing viscosity resulting from a cooling process as curing mechanism.**

**This paper demonstrates the suitability of the T3DP-process for the AM of hard metal compounds. Using WC-Co suspensions with a solid content of 67 vol%, single droplets were deposited and first components manufactured. After de-binding and sintering, completely dense samples were achieved. Zero porosity was determined in the microstructures analyzed by means of FESEM and optical microscopy.**

*Keywords: Additive Manufacturing, Thermoplastic 3D printing, hard metal, cemented carbide, WC-Co*

---

## I. Introduction

Additive Manufacturing (AM) is a manufacturing process that allows the build-up of objects layer-by-layer. Formerly, AM was also referred to as rapid prototyping (RP) or Solid Freeform Fabrication (SFF). In popular science, the term "3D printing" is used as a synonym for Additive Manufacturing. According to ASTM, Additive Manufacturing is a "process of joining material to make objects from 3D model data, usually layer upon layer" [1]. Today, AM of polymers is state-of-the-art. In the field of metals and ceramics, it is possible to process more and more materials.

For hard metal materials, the technical application of AM technologies has so far been limited. First investigations were described by Zong *et al.* in 1992. WC-Co-Ni powder mixtures were processed by means of Selective Laser Sintering (SLS) [2]. Laoui *et al.* used WC-9 wt% Co for SLS and infiltrated the manufactured structures with copper [3], Kruth *et al.* made 3D pyramid parts from WC-12 wt% Co using SLS followed by cobalt infiltration and achieved a maximum density of 89.5 % [4]. The manufacturing of WC-Co composite using SLS followed by Cu infiltration was described by Gu *et al.* [5, 6]. Kumar produced a density of 96 % with non-infiltrated WC-9Co-parts from the SLS-process [7].

The Additive Manufacturing of hard metal components with 3D printing was investigated too. Kelley produced a green density of 52 vol% using a powder-bed-based process and a particle size between 38 µm and 53 µm by using a special densification process for the powder bed [8]. Kernan *et al.* described a suspension-based 3D printing process and achieved a green density of about 47 % of theoretical density for a finer powder mixture, which allowed the realization of a layer thickness of 25 µm [9].

Thermoplastic 3D printing (T3DP) has been developed as an AM technology [10], which can be used for the production of dense ceramic components independent of the physical properties of the used powders (e.g. light absorption) [11] as well as for the production of multi-material-components [12, 13] to combine multi-functional properties with freedom in design and construction [14]. The combination of precise deposition of small droplets with the fast deposition of filaments is one of the main advantages of T3DP. The small droplets enable a high resolution in critical volumes and the deposition of filaments guarantees a high production speed for volumes where no change in material occurs.

The AM of dense alumina components with the use of T3DP could be demonstrated [10] as well as the AM of multi-material components (zirconia-stainless steel) [11, 12]. Molten thermoplastic feedstocks (=suspensions) are processed in a dispensing unit with xyz positioning. The melting temperature of the suspensions (approx. 100 °C) and the viscosity are relatively low compared to the thermoplastic feedstocks that are used in conventional Fused Filament Fabrication (FFF).

The main goal of the presented study was to investigate if the T3DP process would also be adequate for the AM of hard metal components. Here especially the preparation of suitable suspensions and the characterization of their rheological behavior were performed and adapted. The deposition of single droplets was realized and first components manufactured, debinded, and sintered. The sintered samples were characterized based on measurements of density and investigation of FESEM images of cross-sections.

---

[*] Corresponding author: uwe.scheithauer@ikts.fraunhofer.de

## II. Materials and Methods

### *(1) Preparation of suspensions*

The hard metal suspensions were prepared by using a powder mixture of wet-milled nanoscaled WC (WC grade DN3.5/H.C. Starck Tungsten) and a 10 wt% Co (Half Micron/Umicore) as well as small amounts of grain growth inhibitors VC and $Cr_3C_2$ (VC grade HV 160 and $Cr_3C_2$ grade 160/H.C. Starck Tungsten). The powder mixture was first dried and sieve-granulated to a granule size below 315 µm. These loose granules were later dispersed and deagglomerated during the suspension preparation. Thereby a powder content of 67 vol% could be realized within the T3DP suspension. A mixture of paraffin (H&R Wax 54/56, H&R Wax Company) and beeswax (bleached pastilles, DAB) was used as binder system. The binder compound and a dispersing agent were heated up to 100 °C in a heatable ball mill. Then the powder mixture was added and the suspension was homogenized by means of stirring for 2 h at 100 °C.

### *(2) Droplet formation*

A heatable micro dispensing system (Vermes, Germany), a system for single-drop deposition, to deposit the hard metal suspension was used. This system consists of a piezo actor, which is actuated by a control unit, a needle inside a small chamber, which opens and closes a nozzle with a diameter of 150 µm, and a lever system connecting the piezo actor with the needle.

### *(3) Characterization of rheological behavior*

For estimating the shear rates acting in the used micro dispensing system, the inner geometry was measured (gap width: 4 mm) and the velocity of the tappet was calculated (maximum velocity: 20 m/s). Occurring shear rates up to 5000 $s^{-1}$ have been calculated.

For characterizing the rheological behavior of the hard metal suspension, a rheometer (Modular Compact Rheometer MCR 302, Anton Paar, Graz, AUT) adjustable between -25 to 200 °C was used. A cone-plate measurement geometry (gap width 44 µm) ensures homogeneous shear stress distribution. An increasing shear rate from 0.1 to 6000 $s^{-1}$ was applied to measure the flow behavior at different temperatures between 60 °C and 100 °C. The shear rate was predefined as the rotation velocity of the cone against the fixed plate and the shear stress was calculated from the measured torque needed to deform the suspension. The dynamic viscosity was calculated from the shear rate and shear stress and plotted as a function of the shear rate.

### *(4) Debinding and sintering*

The debinding of the samples is a very challenging step because of the thermoplastic behavior of the green samples [12]. To avoid any deformation and any oxidation, debinding was performed in a hydrogen atmosphere with low heating rates of 4 K/h and lower, the samples were sintered in a SinterHIP furnace (FCT, Germany). Dense samples could be prepared by sintering at 1350 °C and 60 bar argon HIP pressure.

### *(5) Characterization of sintered components*

The density of sintered samples was measured according to DIN ISO 3369. The relative density was calculated based on the rule of mixture from the densities of WC, Co $Cr_3C_2$ and VC. Magnetic properties, such as saturation moment and coercivity, were determined according to DIN ISO 3326. For microstructural analysis, the samples were polished down to 1 µm using diamond slurries. Images of the microstructure were taken using a FESEM LEO 982 (Carl Zeiss SMT AG) and optical microscopy.

## III. Results and Discussion

### *(1) Rheological behavior of the suspensions*

An ideal suspension for the TD3P process should have a pseudoplastic behavior at a relatively low viscosity level. That means the suspension shows a shear thinning behavior, which results in low viscosity at high shear rates. This is important for metering small volumes through small geometries at low pressures. In contrast, a high viscosity at a low shear rate is necessary for fixing the suspension at the point of application.

The rheological behavior of the suspension is a quality-changing criteria in many shaping technologies, especially for the manufacturing of ceramic, metal or hard metal components using T3DP. The properties of the suspensions essentially determine the shaping process, in this case the formation of droplets (diameter, roundness, occurrence of satellite droplets), which is important for the realizable resolution and accuracy of manufactured components.

Different graphs are plotted in Fig. 1 to show the dynamic viscosity of the suspension as function of the shear rate and dependent on temperature (range of 60 to 100 °C).

All graphs show a shear thinning behavior. With increasing shear rate, the dynamic viscosity decreases. But all curves show an inflection point, where the negative slope of the graphs increase again. In order to identify the responsible mechanism, the shear stress is plotted against the shear rate in Fig. 2.

The decreasing shear stress at the different shear rates indicates a problem of the measurement setup. At higher shear rates the suspension tore off the measurement equipment and a lower torque was measured. The calculated values of shear stress and viscosity became lower than they would have been if the suspension had stayed on the cone and plate completely.

To discuss the results, the “two-plate model” is used [15]. The suspension is placed between two different plates. The lower one is fixed and the upper one is moved. Ideally the suspension is connected completely to both surfaces and no turbulences occur within the suspension. The model describes the suspension as a sum of many different thin layers which are displaced against each other by the induced deformation force.

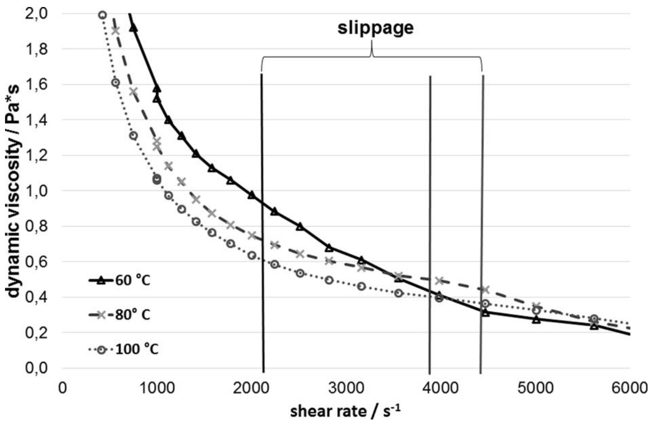

**Fig. 1:** Dynamic viscosity as a function of the shear rate at different temperatures for the hard metal suspension with 67 vol% solid content and shear rates where the slippage started.

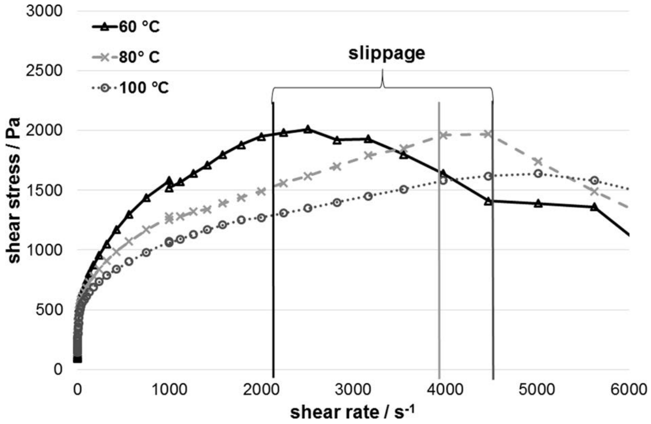

**Fig. 2:** Shear stress as a function of the shear rate at different temperatures for the hard metal suspension with 67 vol% solid content and shear rates where the slippage started.

The torque needed for the displacement of the layers increases with higher shear rates and suspension viscosity. But the adhesion between the suspension and the plates is limited and therefore the suspension tears off one plate at higher deformation forces.

With an increasing temperature, the viscosity of the suspension and the cohesion between the layers decreases and a lower torque is needed to displace the layers. With increasing temperatures the suspension tears off one plate at higher shear rates and the inflection point of the viscosity curve is shifted to higher shear rates.

The lowest dynamic viscosity was measured for the highest temperature. This results from the lubrication effect of the paraffin, which increases with rising temperature.

### *(2) Sintered components*

Figs. 3–7 show two different defect-free sintered test samples. Single walls were manufactured and sintered without any defects or deformation. The elevations at the edges of test Sample 1 result from the used test rig. So far the deposition of droplets and the movement of the axis are not synchronized perfectly yet. Thus the axis slows down on the edges of the manufactured sample but the deposition of the droplets still continues with the same frequency. Therefore more material is deposited than needed and the samples become higher at the edges than in the areas in between.

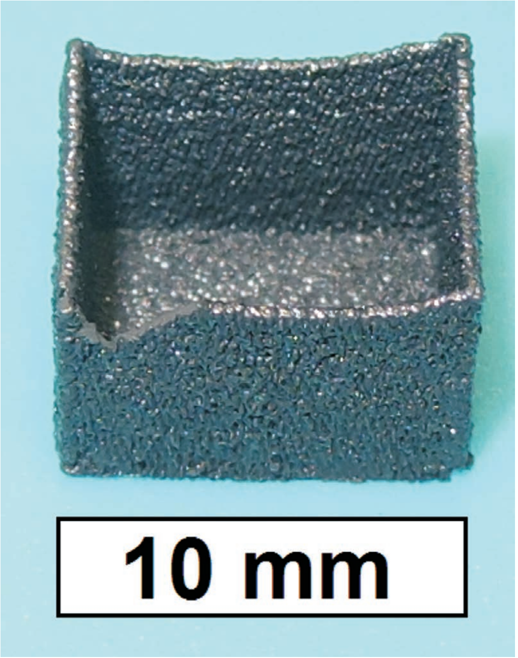

**Fig. 3:** WC-Co test sample 1 manufactured with T3DP.

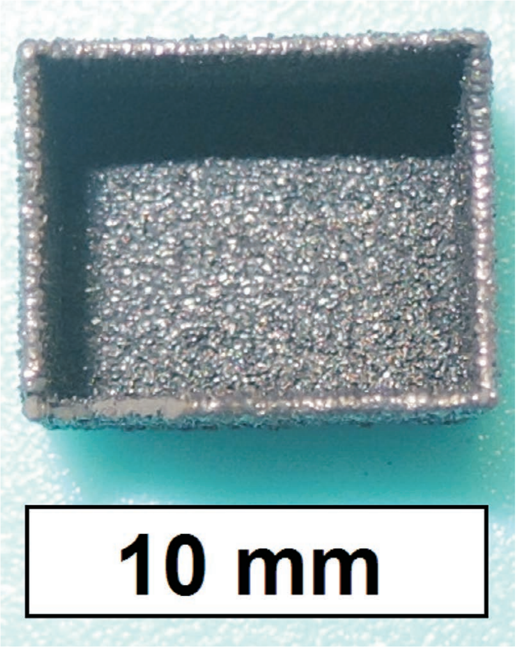

**Fig. 4:** WC-Co test sample 1 manufactured with T3DP – top view.

After being sintered, the components show the typical matt metallic shine of sintered hard metals and no defects or delaminations were detected in a visual inspection.

As seen in Table 1, density values of the printed and sintered sample are 100 % of theoretical density and optical images of polished samples show a pore-free microstructure as shown in Fig. 8 and 9.

**Table 1: Properties of T3D printed or pressed and then sintered hardmetals made from the same starting mixture of WC DN3.5 and 10 wt% Co.**

| sample | density | | Hc | mS | | porosity |
|---|---|---|---|---|---|---|
| [process] | [g/cm$^3$] | [% theor.] | [kA/m] | [μTm$^3$/kg] | [% theor.] | [A-B-C] |
| T3DP | 14.23±0.01 | 100.0 | 47±1 | 15.1±0.3 | 80.7 | 02 – 00 – 00 |
| pressed | 14.22±0.01 | 99.9 | 47±1 | 15.3±0.3 | 81.8 | 02 – 00 – 00 |

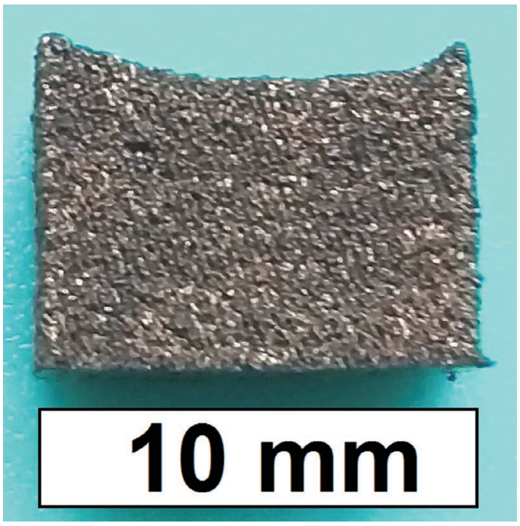

**Fig. 5:** WC-Co test sample 1 manufactured with T3DP – lateral view.

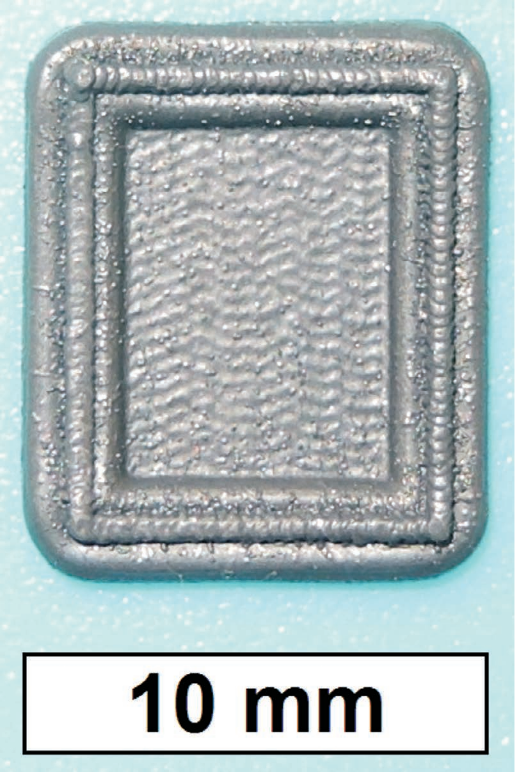

**Fig. 6:** WC-Co test sample 2 manufactured with T3DP – top view.

Magnetic properties are comparable with the same material shaped in a conventional dry pressing process. Magnetic saturation of 15.1 μTm$^3$kg$^{-1}$ corresponds to 81 % of theoretical magnetic saturation, showing that the composition is still within the WC-Co two-phase region and neither free carbon nor etaphase should be present. The coercivity of 47 kA/m corresponds to a nanoscaled grain size of WC grains in the mean size of < 200 nm. The porosity measurement according to ISO 4499 – 4 shows only a limited number of pores < 10 μm and no pores in the range of 10 μm to 25 μm. FESEM images of the microstructure are given in Fig. 10.

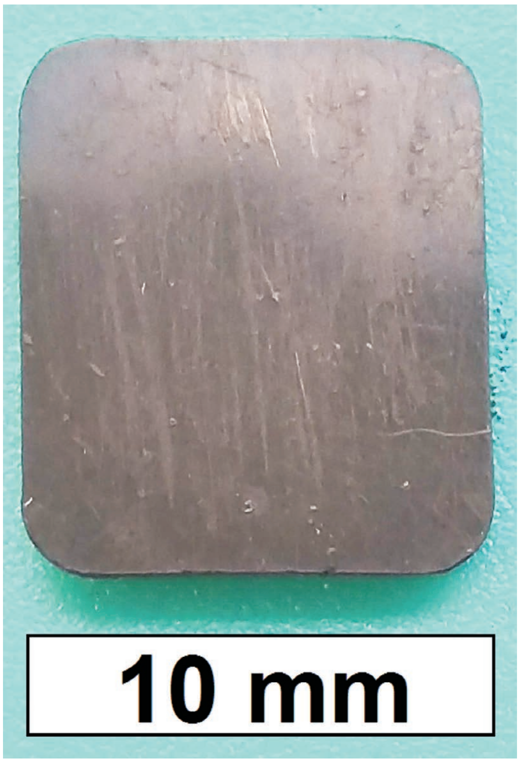

**Fig. 7:** WC-Co test sample 2 manufactured with T3DP – back.

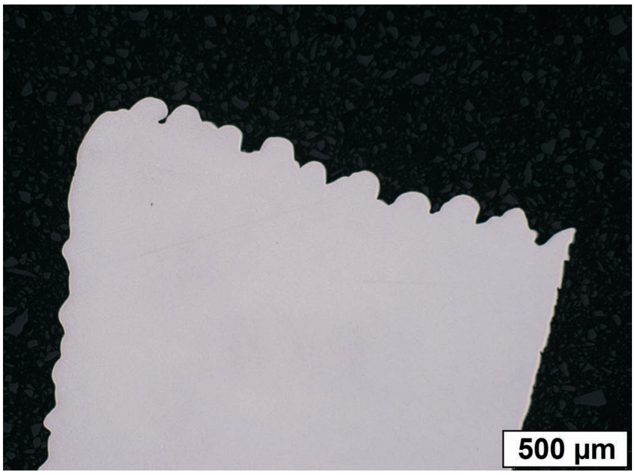

**Fig. 8:** Optical images of sintered hard metal test sample manufactured with T3DP with the as-sintered surface.

The microstructure consists of a homogeneous Co binder phase (dark) and mostly triangular WC grains in the size between 50 nm to 500 nm. Mechanical properties have not been measured so far, but it can be expected that there will be no difference to conventionally shaped hard metal components with the same composition.

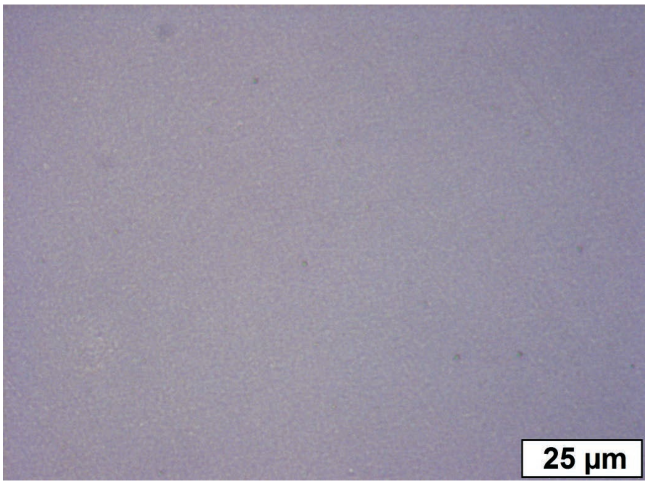

**Fig. 9:** Optical images of sintered hard metal test sample manufactured with T3DP with the pore-free microstructure.

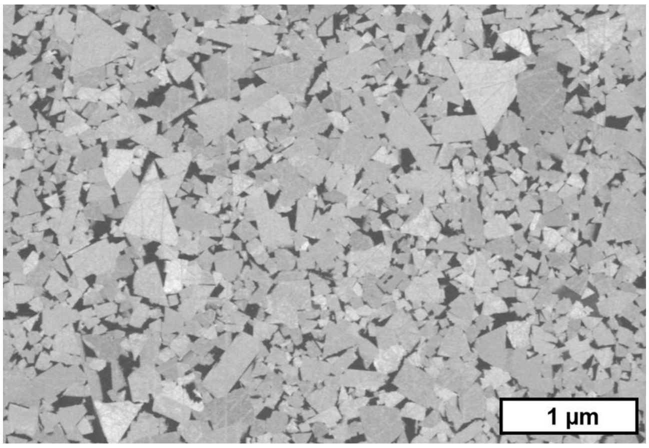

**Fig. 10:** FESEM image of the microstructure of the hard metal part manufactured by T3DP with the composition of WC-10Co-1GGI (grain growth inhibitor).

## IV. Summary and Conclusions

The Thermoplastic 3D printing process has been shown to be suitable for the AM of hard metal components.

A suspension with 67 vol% could be realized and the rheological behavior was characterized. The dynamic viscosity of the thermoplastic suspension increases with decreasing temperature and decreasing shear rates. At shear rates of 5000 $s^{-1}$ and higher, dynamic viscosities of 0.5 Pa·s and lower were measured for all investigated temperatures.

Sintered hard metal components show a dense microstructure and typical magnetic values. With further adjustment and development of Thermoplastic 3D Printing, the production of components with higher geometrical complexity will be possible. However, more work has to be done especially to study a wider range of hard metal compositions and to enhance the understanding of the principle limitations concerning component size, surface roughness and building speed. A very wide range of geometries and compositions should be possible in general, thus allowing for totally new types of tools and applications.

## References

1 ASTM-Standard F2792 – 12a: Standard Terminology for Additive Manufacturing Technologies. March 1, 2012, ASTM International Distributed under ASTM license by Beuth publisher.

2 Zong, G., Wu, Y., Tran, N., Lee, I., Bourell, D.L., Beaman, J.J., Marcus, H.L.: Direct selective laser sintering of high temperature materials, solid freeform fabrication symposium, Austin, 72 – 85, (1992).

3 Laoui, T., Froyen, L., Kruth, J.-P.: Effect of mechanical alloying on selective laser sintering of WC-9Co powder, *Powder Metall.*, **42**, [3], 203 – 205, (2000).

4 Kruth, J.P., Levy, G., Klocke, F., Childs, T.: Consolidation phenomena in laser and powder-bed based layer manufacturing. *CIRP Annals*, **56**, [2], 730 – 759, (2007).

5 Gu, D., Shen, Y.: Influencement of reinforcement weight fraction on microstructure and properties of submicron WC-$Co_p$/Cu bulk MMCs prepared by direct laser sintering, *J. Alloy. Compd.*, **431**, [1 – 2], 112 – 120, (2000).

6 Gu, D., Shen, Y.: WC-Co particulate reinforcing cu matrix composites produced by direct laser sintering, *Mater. Lett.*, **60**, [29 – 30], 3664 – 3668, (2006).

7 Kumar, S.: Manufacturing of WC-Co moulds using SLS machine, *J. Mater. Process. Tech.*, **209**, [8], 3840 – 3848, (2009).

8 Kelley, A.: Tungsten carbide-cobalt by three dimensional printing, Master Thesis, MIT, 1998.

9 Kernan, B.D., Sachs, E.M., Oliveira, M.A., Cima, M.J.: Three-dimensional printing of tungsten carbide-10 wt% cobalt using a cobalt oxide precursor, *Int. J. Refract. Met. H.*, **25**, [1], 82 – 94, (2007).

10 Scheithauer, U., Schwarzer, E., Poitzsch, C., Richter, H.-J., Moritz, T., Stelter, M.: Method for producing ceramic and/or metal components. WO-Patent 2015/177128 A1, (2015).

11 Scheithauer, U., Schwarzer, E., Richter, H.-J., Moritz, T.: Thermoplastic 3D printing – an Additive Manufacturing method for producing dense ceramics, *JACT*, 1 – 6, (2014).

12 Scheithauer, U., Bergner, A., Schwarzer, E., Richter, H.-J., Moritz, T.: Studies on Thermoplastic 3D Printing of steel-zirconia composites, *J. Mat. Res.*, **29**, [17], 1931 – 1940, (2014).

13 Scheithauer, U., Slawik, T., Schwarzer, E., Richter, H.-J., Moritz, T., Michaelis, A.: Additive Manufacturing of metal-ceramic-composites by Thermoplastic 3D-printing, *J. Ceram. Sci. Tech.*, **06**, [02], 125 – 132, (2015).

14 Scheithauer, U., Schwarzer, E., Härtel, A., Richter, H.-J., Moritz, T., Michaelis, A.: Processing of thermoplastic suspensions for Additive Manufacturing of ceramic- and metal-ceramic-composites by Thermoplastic 3D-Printing (T3DP), 11th International Conference on Ceramic Materials and Components for Energy and Environmental Applications, Ceramic Transactions, 258, The American Ceramic Society, (2016).

15 Mezger, T.G.: The Rheology Manual (in German). 5th Edition in german. Vincentz Network, Hanover, 2016.